Enhancing Source Camera Identification Performance With a Camera Reference Phase Sensor Pattern Noise

Xiangui Kang, *Member, IEEE*, Yinxiang Li, Zhenhua Qu, and Jiwu Huang, *Senior Member, IEEE*

***Abstract*—Sensor pattern noise (SPN) extracted from digital images has been proved to be a unique fingerprint of digital cameras. However, SPN can be contaminated largely in the frequency domain by image content and nonunique artefacts of JPEG compression, on-sensor signal transfer, sensor design, color interpolation. The source camera identification (CI) performance based on SPN needs to be improved for small sizes of images and especially in resisting JPEG compression. Because the SPN is modelled as an additive white Gaussian noise (AWGN) in its extraction process from an image, it is reasonable to assume the camera reference SPN to be a white noise signal in order to remove the interference mentioned above. The noise residues (SPN) extracted from the original images are whitened first, then they are averaged to generate the camera reference SPN. Motivated by Goljan *et al.*'s test statistic peak to correlation energy (PCE), we propose to use correlation to circular correlation norm (CCN) as the test statistic, which can lower the false positive rate to be a half of that with PCE. Theoretical analysis shows that the proposed CI method can remove the interference and raise the CCN value of a positive sample and thus achieve greater CI performance, CCN values of the negative sample class with the proposed method follow the normal distribution N (0,1) and the false positive rate can be calculated. Compared with the existing state of the art on seven cameras, 1400 photos totally (200 for each camera), the experimental results show that the proposed CI method achieves the best receiver operating characteristic (ROC) performance among all CI methods in all cases and especially achieves much better resistance to JPEG compression than all of the existing state-of-the-art CI methods.**

***Index Terms*—Camera identification (CI), multimedia forensic, receiver operating characteristic (ROC), sensor pattern noise (SPN), white correlation.**

I. Introduction

NOWADAYS as the digital camera is becoming more and more convenient for photo acquisition, digital images can be found everywhere in today's daily life. Meanwhile, digital images are easy to modify and edit. With an image editing software such as Photoshop, a user can change the image content without leaving any visual witness, which may result in the problem of image forensics. Typical image forensics includes source camera identification, source device linking, integrity verification, authentication, etc. Image forensics, which only relies on the intrinsic feature of the imaging device or the image itself, is becoming more and more important and draws much attention from this research community in recent years [1]–[19].

This paper mainly discusses the image forensic technology based on the sensor pattern noise (SPN). Pattern noise [2], [3] is defined as any noise component that cannot be eliminated by averaging. Due to the manufacturing imperfection and the difference of silicon wafers, the output of the pixels on the sensor may vary from each other even if they are exposed to the same illumination. Therefore, a kind of pattern noise, PRNU, is introduced to every image taken by the camera. Since it is independent of the environment, it is stable and widely exists in all sensor-based cameras. This is the main component of the SPN for digital cameras, so SPN sometimes refers to PRNU directly in some later works.

The camera reference SPN extracted from digital images has been proved to be a unique fingerprint of digital cameras [3]. Source camera identification (CI) can be formulated as the detection of camera reference SPN under hypotheses. Let $\mathbf{y} = \{y_i | i = 0, 1, \ldots, N-1\}$ be the camera reference SPN and $\mathbf{x} = \{x_i\}$ be the noise residue extracted from a test image.

Hypothesis H_0 : $\mathbf{y}$ is not the correct camera reference SPN of the noise residue $\mathbf{x}$ extracted from a test image, i.e., the test image is not taken by the reference camera. In other words, $\mathbf{x}$ is a negative sample for $\mathbf{y}$.

Hypothesis H_1 : $\mathbf{y}$ is the correct camera reference SPN of the noise residue $\mathbf{x}$ extracted from a test image, i.e., the test image is taken by the reference camera. In other words, $\mathbf{x}$ is a positive sample for $\mathbf{y}$.

Lukas and Fridrich *et al.* [3], [5] firstly proposed a popular method to extract camera reference SPN for source CI. The noise residue $\mathbf{w}_k$ is obtained by denoising an original image $\mathbf{I}_k$ with a wavelet denoising filter [3], then the camera reference SPN $\mathbf{y}$ is equal to the average of these noise residues

$$\mathbf{y} = \frac{\sum_{k=0}^{L-1} \mathbf{w}_k}{L} \tag{1}$$

where L denotes the total number of images used for the extraction of camera reference SPN. The normalized correlation coefficient measure the similarity of the noise residue (SPN) $\mathbf{x}$ extracted from a test image $\mathbf{I}$ and the camera reference SPN $\mathbf{y}$ of camera C. If the normalized correlation coefficient is greater than a predefined threshold, image $\mathbf{I}$ is considered to be taken by the camera C, that is, C is deemed as the source camera of image $\mathbf{I}$. The SPN serves as a bullet-scratch for image source tracking. The experimental results in [3], [5] show that the proposed CI

Manuscript received February 13, 2011; revised August 21, 2011; accepted September 04, 2011. Date of publication September 15, 2011; date of current version March 08, 2012. This work was supported by 973 Program under Grant 2011CB302204, by NSFC under Grant 61070167 and Grant U1135001, and by Ph.D. Programs Foundation of Ministry of Education of China under Grant PPFMEC 20110171110042. The associate editor coordinating the review of this manuscript and approving it for publication was Dr. Alex ChiChung Kot.

The authors are with the School of Information Science and Technology, Sun Yat-Sen University, Guangzhou 510006, P. R. China (e-mail: isskxg@mail.sysu.edu.cnq; liyx@student.sysu.edu.cn; qzhua3@gmail.com; isshjw@mail.sysu.edu.cn).

Color versions of one or more of the figures in this paper are available online at http://ieeexplore.ieee.org.

Digital Object Identifier 10.1109/TIFS.2011.2168214

approach is applicable to differentiate two cameras even if they are of the same brand and model. We call the CI approach in [3] the basic SPN CI method or "basic SPN" in short form, the extracted camera reference SPN as basic camera reference SPN in the rest of this paper.

Chen and Fridrich *et al.* [8], [10] proposed a maximum likelihood method to estimate the PRNU's multiplicative factor $\mathbf{K}$ of camera SPN

$$\mathbf{K} = \left(\sum_{k=0}^{L-1} \mathbf{w}_k \mathbf{I}_k\right) \Big/ \left(\sum_{k=0}^{L-1} \mathbf{I}_k \mathbf{I}_k\right) \tag{2}$$

where L is the number of images used in the extraction. The division and multiplication operation between vectors in the equation are element wise, which is the same in the rest of this paper. The camera reference SPN $\mathbf{y}$ for a test image is calculated as

$$\mathbf{y} = \mathbf{IK} \tag{3}$$

where $\mathbf{I}$ denotes the test image. In [8] and [10], the normalized correlation coefficient is used to measure the similarity between the image noise residue $\mathbf{x}$ and the camera C's reference SPN $\mathbf{y}$. Chen and Fridrich *et al.* [8] noted that the periodic structure artefacts of the SPN resulted from color interpolation, on-sensor signal transfer, sensor design [8], are not unique for one specific camera and are shared among the cameras of the same brand or the cameras sharing the same sensor design. They proposed to perform zero-mean operation [8], [16] to the camera reference SPN $\mathbf{y}$ to lessen this effect. They also proposed to perform Wiener filtering to the Fourier magnitude of SPN to lessen the JPEG compression artefacts only when there exist artefacts in the form of visually identifiable patterns. Goljan and Fridrich *et al.* [16], [18] proposed to use peak to correlation energy (PCE) to measure the similarity between $\mathbf{x}$ and camera reference SPN $\mathbf{y}$ in order to suppress the impact of periodic noise contamination and enhance the CI performance. Their CI method [8], [16], [18] is called maximum likelihood estimation camera reference SPN CI method (MLE SPN).

There are some other works dedicated to enhance the SPN extracted from a test image [9] or to improve the camera reference SPN extraction [13], [14]. Li [9] demonstrates that the SPN extracted from a single image can be contaminated by the image scene details such as texture, periodic structure. Their underlying hypothesis is that the stronger a signal component in a SPN, the less trustworthy the component should be, and thus should be attenuated. He proposed five models aiming at attenuating the interference from scene details, each with a user-chosen threshold parameter. The noise residue extracted from a test image is preprocessed directly in spatial domain by each model (equation) before calculating the normalized correlation coefficient. However, attenuating the interference from scene details in spatial domain may also attenuate the useful SPN component.

Hu *et al.* [13] proposed an enhanced method to extract a camera SPN. They assume that the large component of a camera SPN is more reliable and thus should be used in correlation detection while the other components should be discarded. The values of the camera SPN are sorted firstly, then a certain percent, 5% for example, of top values are recorded together with their location information to form the enhanced camera reference SPN for future detection usage. The remaining pixels are set to zero. The SPN extracted from a test image is enhanced according to the location information of the top values in the enhanced camera SPN. That is, only the SPN pixel values at the same location are kept and the rest are discarded. Hu *et al.* in [14] further expanded their work from a single color channel (e.g., green channel) to three color (RGB) channels. Similar to the work in [13], three large component SPNs for three color channels are extracted respectively. If the structure of the CFA used in the camera is known, the *exclusive color assignment rule* is considered to get the exclusive large component SPN for each channel. In other words, only pixel values without interpolation in the large component SPN are kept. At last, the three exclusive large component SPNs are combined to generate the camera reference SPN. However, the CFA structure is usually unknown in practice. The authors used an approximate approach. When constructing the exclusive large component SPN from three large component SPNs of three colors, for a specific pixel, its value is kept if it is the largest among the three color channels at the same location.

Goljan *et al.* [11] extended their previous work to find the source camera of an image even if the image is cropped and scaled down. A two-step search algorithm was used to retrieve the scale factor. The maximum of the normalized cross-correlation of two signals is used to retrieve the cropping parameters. The experimental results show that the proposed approach works for images linearly scaling down to 0.5, or cropped by more than 90%. The fact that SPN can be used as a template for the retrieval of image geometric transformation parameters is useful in resynchronization of digital watermark. The approach can also be used in the scenario where a test image is maliciously edited to avoid source camera identification [11]. Goljan *et al.* [17] also proposed several methods to speed up the search of camera SPN fingerprint database.

Besides the application of source camera identification, SPN can also serve as a kind of watermark for image forgery detection. Chen and Fridrich *et al.* [8], [10] proposed a method based on the fact that forgery operations such as object copy-move will change or destroy the camera reference SPN in the forgery area. This is true if the forged object is from another camera or the spatial location is changed when compared to its source image. In order to perform forgery detection on a full size image, a full size camera reference SPN is extracted first. Then, a specific size of window, say 128×128 pixels, slides in both of the SPN of the test image and the camera reference SPN with the same step and direction, performing correlation between the two windows. If the correlation coefficient is smaller than the predefined threshold which is obtained by performing the Neyman-Pearson hypothesis testing on the statistic data of the correlation coefficients, the centre pixel of the window in the test image at the same position is marked as a forged pixel. When the window slides over the whole SPN, the forged area will appear in the test image. At last, some successive operations such as dilating are used to make the result more accurate. The experimental results show that this method can reveal forgery operations, such

as copy-move, object removing within an image or object insertion from another image.

Although there are some works dedicated to improve the performance of source camera identification based on SPN up to now, no comparison of receiver operating characteristic (ROC) curve for kinds of source camera identification was given in the existing works. All of the artefacts mentioned above may result in a performance drop for source camera identification. To our best knowledge, the effective method to enhance camera reference SPN in the frequency domain aiming at removing the interference from scene details and camera signal processing is currently lacking. The identification performance needs to be improved for small sizes of images and especially in resisting JPEG compression [3], [6]–[9], [17]. In this paper, we propose a camera reference phase SPN to enhance the ROC performance of source camera identification. The contamination from the image details, JPEG compression and camera signal processing is removed, and the false positive detection triggered by the correlation with any other camera SPN is eliminated, thus negative data class and positive data class can be separated. Both theoretical analysis and extensive experiments show that the proposed CI method achieves the best ROC performance among all CI methods especially in resisting JPEG compression.

The rest of this work is organized as follows. In Section II we will introduce a camera reference phase SPN and propose a novel test statistic-correlation over circular correlation norm (CCN) for CI. Theoretical analysis of our proposed scheme is given in this section. Section III will show the experimental results compared with the state-of-the-art works. The conclusion is made in Section IV.

II. Camera Reference SPN Extraction and Detection

A. Camera Reference SPN Extraction

The SPN (noise residue) extracted from a single image can be contaminated largely in the frequency domain by image detail from scene and nonunique artefacts of on-sensor signal transfer, sensor design, and color interpolation. The periodic structures or texture will result in large Fourier magnitude for some frequency components. Fig. 1 shows that the image SPN (noise residue extracted from an image) can be contaminated by the image details, causing some large frequency magnitude coefficients. Because the SPN (noise residue) is modelled as an additive white Gaussian noise (AWGN) in its extraction process with a wavelet-based denoising filter [20], it is reasonable to assume the camera reference SPN to be a white noise signal with flat frequency spectrum in order to remove the impact of the contamination in the frequency domain from the image details and the camera signal processing mentioned above. The noise residue extracted from an original image $\mathbf{I}_k$ is $\mathbf{w}_k = \mathbf{I}_k - F(\mathbf{I}_k)$, where $F(\mathbf{I}_k)$ denotes the denoised image. Then $\mathbf{w}_k$ is whitened firstly in the frequency domain and has constant Fourier magnitude coefficients except that its direct current (dc) Fourier coefficient equals zero. We obtain its phase-only component $\mathbf{W}_{\phi k}$

$$\begin{aligned} \mathbf{W}_k &= \mathrm{DFT}(\mathbf{w}_k) \\ \mathbf{W}_{\phi k} &= \mathbf{W}_k / |\mathbf{W}_k| \end{aligned} \tag{4}$$

where $|\mathbf{W}_k|$ is the Fourier magnitude of $\mathbf{W}_k$.

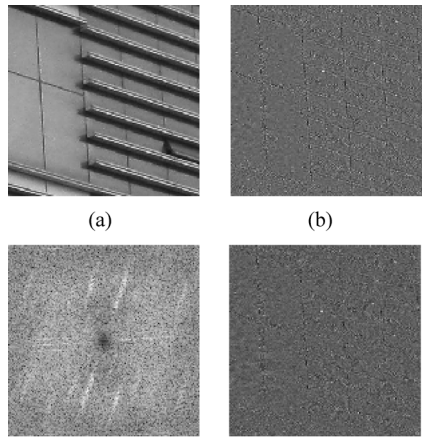

Fig. 1. (a) Image taken by a Canon PowerShot A3000 IS. (b) SPN $\mathbf{w}$ extracted from (a). (c) Fourier magnitude spectrum of (b). (d) Phase-only component $\mathbf{w}_\phi$ in spatial domain.

The camera reference SPN $\mathbf{y}$ is obtained by averaging the phase-only component $\mathbf{W}_{\phi k}$ and performing inverse DFT

$$\mathbf{y} = \mathrm{real}\left(\mathrm{IDFT}\left(\frac{\sum_{k=0}^{L-1}\mathbf{W}_{\phi k}}{L}\right)\right) \tag{5}$$

where L denotes the total number of images used in the extraction, real() means that only the real part is kept because the imaginary part is very small and can be ignored. We call $\mathbf{y}$ in (5) the camera reference phase SPN or phase SPN in the rest of the paper. Note that the periodic noise component and linear pattern [18] in $\mathbf{y}$ is removed and the impacts of the contaminations in the frequency domain from the image detail and the camera signal processing mentioned above is removed, thus the negative sample class and positive sample class can be separated. In the next section, we will give a theoretical analysis to show that the reference phase SPN $\mathbf{y}$ also raises the test statistic of the positive sample. The more images are used to extract the camera reference phase SPN, the more obvious is the advantage of the camera reference phase SPN over the basic camera reference SPN and the MLE camera reference SPN.

Note that $\mathbf{y}$ is a white noise signal. Its circular correlation is a delta function $\delta(m)$

$$r_{\mathbf{y}}(m) = \frac{1}{N}\sum_{i=0}^{N-1} y_i y_{i\oplus m} = \delta(m). \tag{6}$$

The operation $\oplus$ is modulo N addition in $\mathbb{Z}_N$. According to (6), $\mathbf{y}$ is only correlated with itself. That is, only at $m = 0, r_{\mathbf{y}}(0) \neq 0$. For $m \neq 0, r_{\mathbf{y}}(m) = 0$.

According to the assumption made by Fridrich and Goljan [18, p. 8], the mean of squared normalized correlation between image noise residue (SPN) $\mathbf{y}$ and other than correct camera SPN $\mathbf{x}$ (hypothesis H_0) can be estimated by the mean of squared correlation of image noise residue (SPN) $\mathbf{y}$ and the correct but shifted version $\mathbf{y}_m = \{y_{i\oplus m}\}$. It can be formulated as

$$E(\rho^2(\mathbf{x},\mathbf{y})) = c \times E(r_{\mathbf{y}}^2(m)), m \neq 0 \tag{7}$$

where c is a constant. Under hypothesis H_0, according to (7), if $r_{\mathbf{y}}(m) = 0, m \neq 0, E(\rho^2(\mathbf{x},\mathbf{y})) = 0, \rho(\mathbf{x},\mathbf{y}) = 0, r_{\mathbf{xy}}(0) = (1)/(N)\sum_{i=0}^{N-1} x_i y_i = 0$. That is, the SPN $\mathbf{y}$ is uncorrelated with any other camera SPN $\mathbf{x}$. Although the assumption (7) may not be perfectly satisfied [18], it provides good insight into the advantage that the camera reference phase SPN is theoretically unique in terms of that the false positive detection triggered by the correlation with any other camera reference SPN is eliminated. Note that the number of other cameras can be of thousands and tens of thousands, and the other cameras can be of the same or different brand with the reference camera, and can be of the same or different manufactory with the reference camera, so it is important to avoid this kind of false positive detection in practice.

B. Camera Reference SPN Detection

The normalized correlation coefficient can be used as the test statistic [3], [8], [9]. Vectors $\mathbf{x}$ and $\mathbf{y}$ are always preprocessed to have zero mean to avoid the impact of deviation [18], so both $\mathbf{x}$ and $\mathbf{y}$ are two signal vectors in $\mathbb{R}^N$ with zero mean. In this paper, all SPN related vectors are assumed to have zero-mean without specific claim. The normalized correlation coefficient $\rho(\mathbf{x},\mathbf{y})$ between the image noise residue $\mathbf{x}$ and the camera C's reference SPN $\mathbf{y}$ is defined as

$$\rho(\mathbf{x},\mathbf{y}) = \frac{\mathbf{xy}}{\|\mathbf{x}\|\|\mathbf{y}\|} \tag{8}$$

where matrix multiplication $\mathbf{xy} = \sum_{i=0}^{N-1} x_i y_i$, $\|\mathbf{x}\|$ is the norm of $\mathbf{x}$

$$\|\mathbf{x}\| = \sqrt{\mathbf{xx}} = \sqrt{\sum_{i=0}^{N-1} x_i^2}.$$

Under hypothesis H_0 and if $\mathbf{x}$ is independent with $\mathbf{y}$, the distribution of $\rho(\mathbf{x},\mathbf{y})$ is a Gaussian distribution with zero mean and $1/N$ variance [18]. With a detection threshold $\rho(\mathbf{x},\mathbf{y}) = (t_0)/(\sqrt{N})$, the false positive rate with $\rho(\mathbf{x},\mathbf{y})$ is $Q(t_0)$ where $Q()$ is the complementary cumulative density function of a normal random variable N (0,1).

Goljan *et al.* [16], [18] proposed another detection statistic, peak to correlation energy (PCE), to measure the similarity between $\mathbf{x}$ and $\mathbf{y}$. The circular shift vector is $\mathbf{y}_m = \{y_{i\oplus m}\}$ where the operation $\oplus$ is modulo N addition in $\mathbb{Z}_N$. The circular cross-correlation $r_{\mathbf{xy}}(m)$ is defined as

$$r_{\mathbf{xy}}(m) = \frac{1}{N}\mathbf{x}\mathbf{y}_m = \frac{1}{N}\sum_{i=0}^{N-1} x_i y_{i\oplus m}. \tag{9}$$

PCE is defined as

$$\mathrm{PCE} = \frac{r_{\mathbf{xy}}^2(0)}{\frac{1}{N-|\mathrm{A}|}\sum_{m\notin \mathrm{A}} r_{\mathbf{xy}}^2(m)} \tag{10}$$

where A is a small neighbor area around zero where $r_{\mathbf{xy}}(0) = (1)/(N)\mathbf{xy} = (1)/(N)\sum_{i=0}^{N-1} x_i y_i$, $|\mathrm{A}|$ is the size of A. If $\mathbf{x}$ and $\mathbf{y}$ are contaminated by the similar periodic noise which is not unique for one specific camera [18], the circular cross-correlation $r_{\mathbf{xy}}(m)$ may peak for many m values, thus raise the denominator of PCE and PCE drops, and may avoid triggering a false positive identification. That is, PCE achieves the advantage of suppressing periodic noise contamination. If either $\mathbf{x}$ or $\mathbf{y}$ is $i.i.d$ vector or white noise signal, we can prove (please refer to White Correlation Theorem in the Appendix)

$$\mathrm{PCE} = N\rho^2(\mathbf{x},\mathbf{y}) \approx (\sqrt{N}\rho(\mathbf{x},\mathbf{y}))^2. \tag{11}$$

Although PCE has the advantage of suppressing periodic noise contamination [16], [18], it also increases the false positive rate because the square operation to $\rho(\mathbf{x},\mathbf{y})$, as shown in (11), turns a negative correlation $\rho(\mathbf{x},\mathbf{y})$ to a positive PCE value. With a detection threshold $\rho(\mathbf{x},\mathbf{y}) = (t_0)/(\sqrt{N})$, the false positive rate of PCE is $2Q(t_0)$ according to (11), i.e., the false positive rate is doubled with detection statistic PCE.

Motivated by their work, we propose to use the correlation over circular cross-correlation norm (CCN) to suppress the impact of periodic structure noise contamination. The correlation over circular CCN is defined as

$$\begin{aligned} c(\mathbf{x},\mathbf{y}) &= \frac{\mathbf{xy}/N}{\sqrt{\frac{1}{N-|\mathbf{A}|}\sum_{m\notin\mathbf{A}} r_{\mathbf{xy}}^2(m)}} \\ &= \frac{r_{\mathbf{xy}}(0)}{\sqrt{\frac{1}{N-|\mathbf{A}|}\sum_{m\notin\mathbf{A}} r_{\mathbf{xy}}^2(m)}}. \end{aligned} \tag{12}$$

If $\mathbf{x}$ is independent with $\mathbf{y}$, it can be proved (see the White Correlation Theorem in the Appendix) that $E(c(\mathbf{x},\mathbf{y})) = 0, D(c(\mathbf{x},\mathbf{y})) = 1$, where E () is the expectation operation and D () is the variance operation. According to the central limit theorem, $c(\mathbf{x},\mathbf{y})$ follows the normal distribution N (0,1). In Section III, it is demonstrated by the experimental data of the phase SPN CI method, as shown in Fig. 6. Let t_0 be a predefined threshold of $c(\mathbf{x},\mathbf{y})$, the false positive rate can be estimated by

$$p_{\mathrm{fp}} = Q(t_0). \tag{13}$$

The false positive rate with $c(\mathbf{x},\mathbf{y})$ is equal to that with detection statistic $\rho(\mathbf{x},\mathbf{y})$, however $c(\mathbf{x},\mathbf{y})$ achieves the same advantage of suppressing periodic noise contamination as PCE [18]. Our extensive experiments also show that $c(\mathbf{x},\mathbf{y})$ is better than both of $\rho(\mathbf{x},\mathbf{y})$ and PCE.

It can be proved that (see the White Correlation Theorem in the Appendix)

$$\begin{aligned} \frac{1}{N-|\mathbf{A}|}\sum_{m\notin\mathbf{A}} r_{\mathbf{xy}}^2(m) \approx \frac{1}{N^3}\|\mathbf{x}\|^2\|\mathbf{y}\|^2 \\ +\frac{1}{N}\sum_{m=1}^{N-1} r_{\mathbf{x}}(m) r_{\mathbf{y}}(m). \end{aligned} \tag{14}$$

As we know, the circular correlation of one image generally is not less than 0. Both $\mathbf{x}$ and $\mathbf{y}$ are extracted from images, and some linear pattern [18] or JPEG compression block artefacts exist in $\mathbf{y}$ and $\mathbf{x}$, $r_{\mathbf{y}}(m)$ and $r_{\mathbf{x}}(m)$ may

TABLE I
CAMERAS USED IN EXPERIMENTS, SENSOR TYPE, RESOLUTION AND IMAGE FORMAT

Camera Brand	Sensor	Native Resolution	Image Format
Canon PowerShot A3000 IS	1/2.3'' CCD	3648x2736	JPEG
Canon PowerShot A610	1/1.8'' CCD	2592x1944	JPEG
Canon PowerShot A620	1/1.8'' CCD	3072x2304	JPEG
Panasonic Lumix DMC-FZ30	1/1.8'' CCD	3264x2448	JPEG
Nikon D300	23.6×15.8mm CMOS	4288x2848	JPEG
Nikon D40	23.7×15.6 mm CCD	3040x2012	NEF(raw)
Minolta A2	2/3'' CCD	3272x2454	MRW(raw)

peak for many m values, so it is reasonable to consider that the term $(1)/(N)\sum_{m=1}^{N-1} r_{\mathbf{x}}(m)r_{\mathbf{y}}(m) \geq 0$. When either $\mathbf{x}$ or $\mathbf{y}$ is a white noise signal, i.e., $r_{\mathbf{y}}(m) = 0$, for all $m \neq 0$ or $r_{\mathbf{x}}(m) = 0$, for all $m \neq 0$, according to (14), $(1)/(N - |\mathbf{A}|)\sum_{m\notin\mathbf{A}} r_{\mathbf{xy}}^2(m)$ achieves its minimum value $(1)/(N^3)\|\mathbf{x}\|^2\|\mathbf{y}\|^2)$

$$\frac{1}{N-|\mathbf{A}|}\sum_{m\notin\mathbf{A}} r_{\mathbf{xy}}^2(m) \approx \frac{1}{N^3}\|\mathbf{x}\|^2\|\mathbf{y}\|^2 \tag{15}$$

and we have

$$c(\mathbf{x},\mathbf{y}) \approx \sqrt{N}\rho(\mathbf{x},\mathbf{y}). \tag{16}$$

When $\mathbf{y}$ is a white noise signal, the phase-only component of the vector $\mathbf{y}$ is $\mathbf{y}_\phi$, we can have $\mathbf{y} = \mathbf{y}_\phi$, and

$$r_{\mathbf{xy}_\phi}(0) = \mathbf{x}\mathbf{y}_\phi/N = \mathbf{x}\mathbf{y}/N = r_{\mathbf{xy}}(0). \tag{17}$$

Because $r_{\mathbf{y}}(m) = 0$, *for all* $m \neq 0$, the term

$$\frac{1}{N}\sum_{m=1}^{N-1} r_{\mathbf{x}}(m)r_{\mathbf{y}}(m) = 0. \tag{18}$$

The term $(1)/(N-\|\mathbf{A}\|)\sum_{m\notin\mathbf{A}} r_{\mathbf{xy}}^2(m)$ achieves its minimum value $(1)/(N^3)\|\mathbf{x}\|^2\|\mathbf{y}\|^2)$, thus $c(\mathbf{x},\mathbf{y})$ of a positive sample increases. Either $\mathbf{x}$ or $\mathbf{y}$ is assumed to be a white noise signal before calculating the similarity (correlation) measure CCN, we call this correlation **white correlation** (mixed correlation CI method in [12] where the phase-only component of $\mathbf{x}$ is used for correlation calculation is one kind of white correlation). From the above analysis, the white correlation method, such as this proposed phase SPN CI method and the mixed correlation CI method in [12], can theoretically minimize the denominator of detection statistic CCN, thus raise the CCN value of a positive sample, especially in the case where there exist JPEG compression artefacts and linear pattern contamination in the extracted SPN. Recall that under hypothesis $\mathrm{H}_0, c(\mathbf{x},\mathbf{y})$ follows the normal distribution N (0,1). On the other hand, if $\mathbf{y}$ (or $\mathbf{x}$) is a white noise signal, the artefacts and linear pattern contamination [8] have little effect on discriminating a positive sample class and a negative sample class because $r_{\mathbf{xy}_\phi}(0) = r_{\mathbf{xy}}(0)$ (17) and $(1)/(N)\sum_{m=1}^{N-1} r_{\mathbf{x}}(m)r_{\mathbf{y}}(m) = 0)$ (18). That is, the interference between positive sample class and negative one is removed. In practice, the CI with camera reference phase SPN achieves better CI performance than the mixed correlation CI method with white noise signal $\mathbf{x}$ [12]. The reason is that the camera reference phase SPN in this manuscript has the advantages over the basic camera reference SPN [3]. The proposed camera reference phase SPN extraction method as shown in (4) and (5) removes the periodic noise component and other non-white noise contamination in the camera reference SPN, while averaging the noise residues to obtain the basic camera reference SPN adopted in [12] does not remove these contaminations which are not unique for identification of one specific camera. So we adopt the camera reference phase SPN CI method in this paper. The reader interested in mixed correlation CI method is referred to our previous work [12].

In brief, the proposed camera reference phase SPN CI method ("phase SPN") is as follows: 1) Select the flat original images (such as the sky images etc.) to extract the camera reference phase SPN $\mathbf{y}$ as shown in (4) and (5); 2) Calculate the detection statistic $c(\mathbf{x},\mathbf{y})$ between the camera reference SPN $\mathbf{y}$ and the noise residue $\mathbf{x}$ extracted from a test image.

III. EXPERIMENTAL RESULTS

In this section, we will examine the ROC performance of the proposed source camera identification method. In signal detection theory, a ROC curve is a graphical plot of the true positive rate (TPR) versus false positive rate (FPR), for a binary classifier system as its discrimination threshold is varied. The test image SPN $\mathbf{x}$ and the camera reference SPN $\mathbf{y}$ are extracted from green channel. A wavelet-based denoising filter F [3] is used, where F accepts a parameter—the variance of the white Gaussian noise that it removes. We set this variance at 25 for an 8-bit image [3]. We choose the detection statistic *CCN* $c(\mathbf{x},\mathbf{y})$ to measure the similarity between $\mathbf{x}$ and $\mathbf{y}$. The size of A is chosen to be a block of 11×11 pixels. We compare our proposed scheme with the popular CI method—basic SPN CI method in [3]. The basic camera reference SPN $\mathbf{y}$ is obtained by averaging the noise residues extracted from the original images [3], and the image noise residue $\mathbf{x}$ is extracted from a test image and no further preprocession is applied to $\mathbf{x}$ before the calculation of detection statistic $c(\mathbf{x},\mathbf{y})$.

We also compare the proposed CI scheme with the state-of-the-art works: MLE SPN CI method [8], [16], [18] ("MLE SPN" in short form) and Li's model-based CI approaches [9]. We choose two of Li's model-based approaches, "Model 3" and "Model 5" [9], because they show better (or equivalent) results than the other model based approaches in Li's work. The

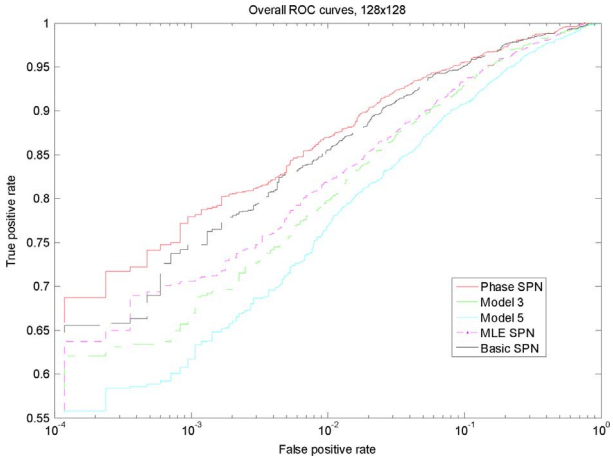

Fig. 2. *Overall ROC curves* of different CI methods on a test image with size of 128 × 128 pixels.

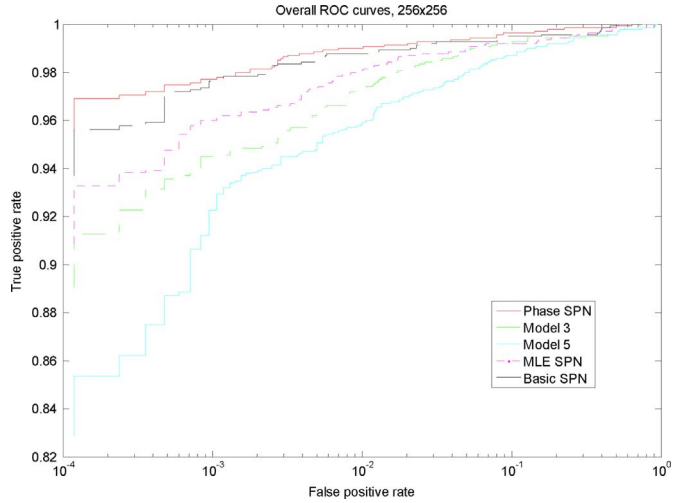

Fig. 3. *Overall ROC curves* of different CI methods on a test image with size of 256 × 256 pixels.

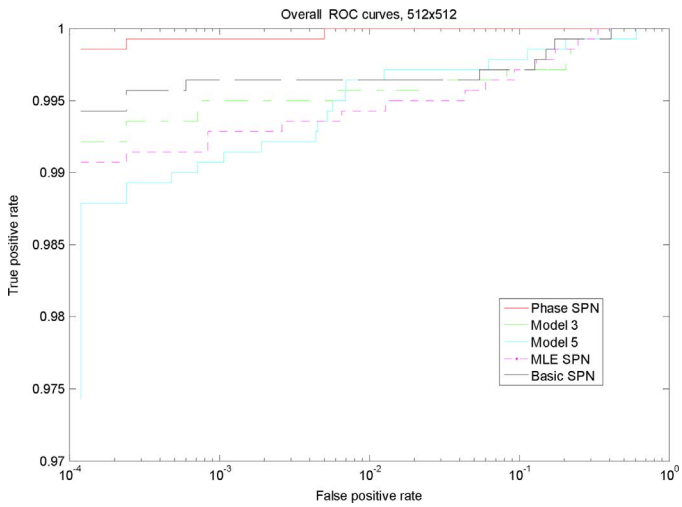

Fig. 4. *Overall ROC curves* of different CI methods on a test image with size of 512 × 512 pixels.

model parameters are chosen the same as that in Li's work. Here Models 3 and 5 denote that before being used for detection, the image noise residue extracted from a test image is preprocessed by model 3 and model 5, respectively, to obtain $\mathbf{x}$. The basic camera reference SPN extraction method is used to obtain the camera reference SPN $\mathbf{y}$. For Fridrich *et al.* MLE SPN CI method [8], [16], [18], the noise residue $\mathbf{x}$ is extracted from a test image $\mathbf{I}$, the camera reference SPN $\mathbf{y} = \mathbf{IK}$, where the camera PRNU factor $\mathbf{K}$ is obtained with maximum-likelihood estimation. Then matrix zero-mean preprocessing [16] is applied to $\mathbf{y}$ to subtract its column mean and row mean, then obtain a renewed $\mathbf{y}$ for CCN calculation.

If CCN $c(\mathbf{x}, \mathbf{y})$ between the test image SPN $\mathbf{x}$ and the camera reference SPN $\mathbf{y}$ is greater than the varying threshold, we make a positive decision that the image is taken by the reference camera, otherwise a negative decision is made. True positive is the correct positive decision under hypothesis H_1. False positive is the positive decision under hypothesis H_0.

Table I shows the image format, native resolution (full size) and imaging sensor property of the cameras used in the experiments. All photos are in JPEG format with the highest JPEG quality factor provided by the camera, except in raw data format for Nikon D40 and Minolta A2. For each camera we have two subimage datasets which are the test image dataset and the original image dataset, respectively. The original image dataset is used for camera reference SPN extraction. The original images are taken on a sunny day of the blue sky whose content is flat or near flat. The test images are taken under a variety of environments, from indoor furniture to outdoor sight. The test image dataset is used as test images for source camera identification. Source camera identification experiment is performed on the image block with different sizes from 128 × 128 to 1024 × 1024. The image block is cropped from the centre of the full size photo.

In order to draw the source camera identification ROC curve, the camera reference SPN is extracted first using $L = 100$–200 original images from the original image dataset for each camera. Then 200 test images taken by this camera are selected as positive samples while 1200 test images taken by the other six cameras (200 for each camera) are selected as negative samples. For each camera we will get 200 positive sample correlation values and 1200 negative sample correlation values. To obtain the *overall ROC curve*, for a given detection threshold, we count the number of true positive decisions and the number of false positive decisions for each camera respectively, and then sum them up to obtain the total number of true positive decisions and false positive decisions. Then, the total TPR and total FPR are calculated to draw the *overall ROC curve*.

Fig. 2 shows the *overall ROC curves* of five methods on image of 128 × 128 pixels cropped from the centre of the 1400 photos in the test image dataset. Figs. 3 and 4 show the results for image size of 256 × 256 and 512 × 512 pixels respectively. In order to show the detail of the ROC curves with low FPR, the horizontal axis of the ROC curve is in logarithmic scale. Table II shows the TPR of the five methods at zero experimental FPR. The TPR of the "phase SPN" method is 99.9% on an image with size of 512 × 512 pixels at zero FPR. The proposed method raises the TPR from 55.9% (MLE SPN) to 65.9% (Phase SPN) at zero experimental FPR on an image block of 128 × 128

TABLE II
TPR OF FIVE METHODS AT ZERO EXPERIMENTAL FPR

Image size(pixels)	Phase SPN	MLE SPN [16]	Basic SPN [3]	Model 3 [9]	Model 5 [9]
128x128	0.659	0.559	0.647	0.584	0.556
256x256	0.956	0.909	0.937	0.891	0.829
512x512	0.999	0.991	0.994	0.992	0.974

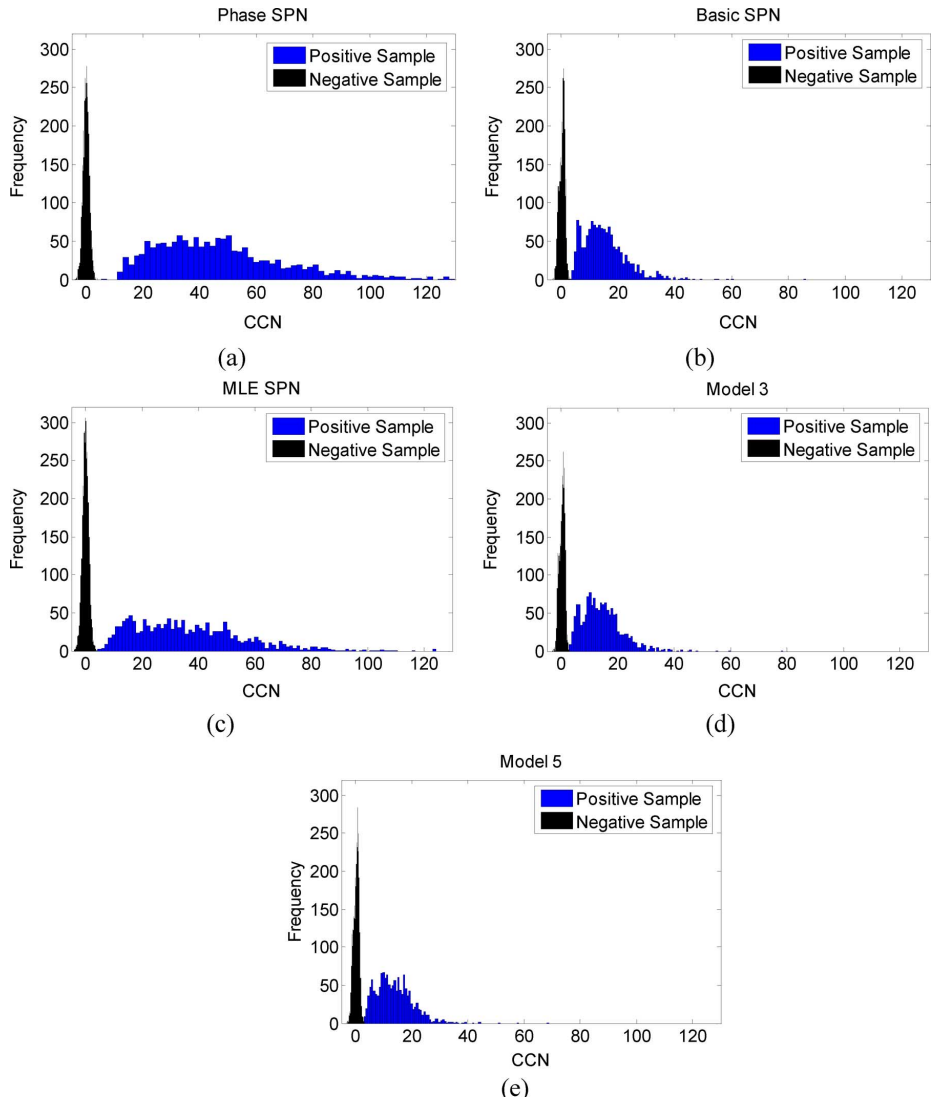

Fig. 5. (a) Histograms of the CCN value of the proposed phase SPN method, (b) basic SPN method, (c) MLE SPN method, (d) Model 3 method, and (e) Model 5 method.

pixels. The TPR of the "phase SPN" is always the largest among the five CI methods no matter what the image size is. The experimental results show that the proposed CI method always outperforms all of the other CI methods and improves the ROC performance of source camera identification, especially increasing the TPR in the case of trustworthy identification which is with a low FPR.

Fig. 5 shows the histogram of the CCN values of the proposed phase SPN CI method, basic SPN CI method, MLE SPN CI method, Li's Model 3 and Model 5 CI method, respectively. The test image size is 1024×1024 pixels. It is observed that the CCN values of the positive data class and negative data class with the phase SPN CI method can be separated successfully, as shown in Fig. 5(a). And there exists a margin between the two classes, the minimum CCN value of the positive data class is 5.4 (the corresponding image contains a large portion of white pixels, i.e., saturated pixels), the largest CCN of the negative data class is 3.9. The average CCN value (47.5) of the positive data class is much larger than all of the other CI methods. The average CCN value of the positive data class with the Basic SPN, MLE SPN, Model 3 and Model 5 method is 15.2, 36.6, 14.4 and 14.0, respectively, and the CCN values of the positive data class and negative data class cannot be separated for each of the other five CI methods. This improvement is mainly due to the proposed camera reference phase SPN. The histogram of the CCN values of the negative data class for the phase SPN

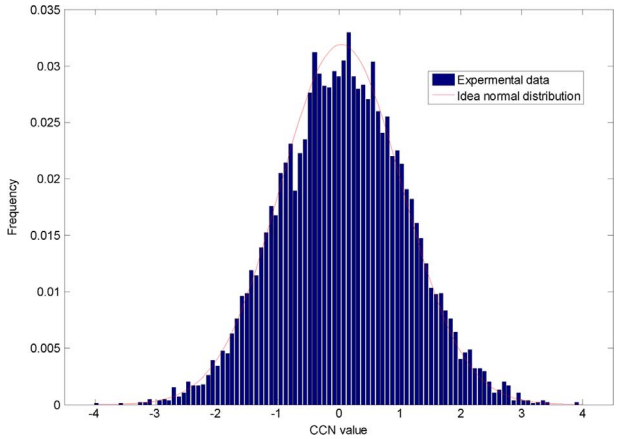

Fig. 6. Histogram of the CCN values of the negative data class with phase SPN CI method fits normal distribution.

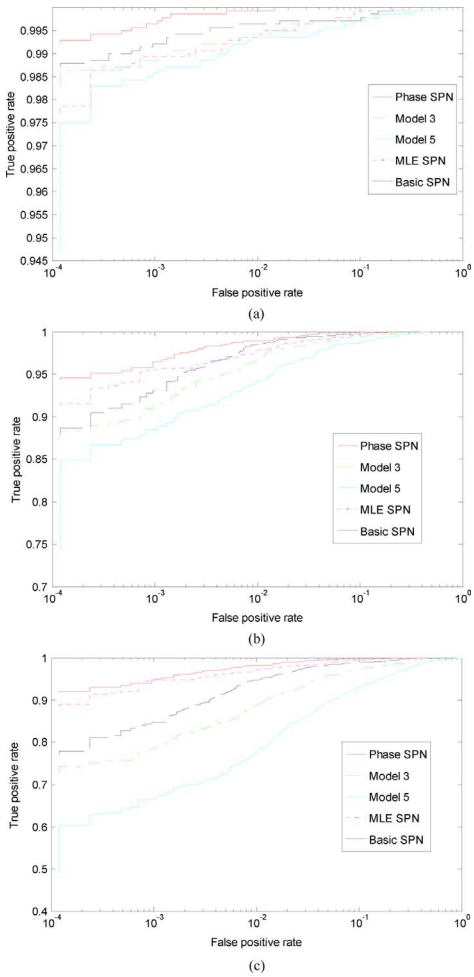

Fig. 7. *Overall ROC curves* of different CI methods on a 512 × 512 JPEG compressed image with different QF: (a) JPEG_90, (b) JPEG_75, (c) JPEG_50.

CI method fits idea normal distribution very well, as shown in Fig. 6. In Fig. 6, the red line denotes the idea normal distribution. It shows that under hypothesis H_0, we can estimate the false positive rate of the phase SPN CI method using (13) in practice. When the image is JPEG compressed, the SPN becomes weak. Fig. 7 shows the overall identification ROC curves on a JPEG compressed image with size of 512 × 512 pixels. The results with size of 1024 × 1024, 256 × 256, 128 × 128 are similar. The test image SPN is extracted from the JPEG compressed (or recompressed) test image with quality factor (QF) being 90% [JPEG_90 in Fig. 7(a)], 75% [JPEG_75 in Fig. 7(b)] and 50% [JPEG_50 in Fig. 7(c)] respectively. The camera reference SPN is extracted from the original image dataset for each camera, which is the same as that in Figs. 2–5. Table III shows the corresponding TPR at the zero experimental FPR on a JPEG compressed image with different QF. The experiment result shows that our proposed phase SPN CI method has much more advantages in resisting JPEG compression than all of the existing state of the art CI methods. This significant improvement is attributed mainly to that the white correlation removes the impact of JPEG artefact contaminations.

IV. Conclusion

In this paper, we examine and compare source camera identification performance from the aspect of ROC curve, and the main contributions of this paper are as follows.

1) Motivated by Fridrich *et al.*'s work, we propose a novel detection statistic CCN which can lower the false positive rate to be a half of that with PCE. Our extensive CI experiments also show that CCN is better than both of the normalized correlation coefficient and PCE. Under hypothesis H_0, CCN value of the phase SPN CI method follows the normal distribution N (0,1), the false positive rate with CCN is given in (13).
2) We introduce a novel camera reference phase SPN as shown in (4) and (5). The contamination from the image details, JPEG compression and the camera signal processing is removed, and the false positive detection triggered by the correlation with any other camera reference SPN is eliminated, the detection statistic of a positive sample is also raised, thus the negative data class and positive data class can be separated more exactly.
3) Both theoretical analysis and extensive experiments show that the proposed CI method achieves the best ROC performance among all CI methods in all cases and especially achieves much better resistance to JPEG compression than all of the existing state of the art CI methods.

Appendix

Proof of White Correlation Theorem:

White Correlation Theorem: Let $\mathbf{y} = \{y_i | i = 0, 1, \ldots, N-1\}$ and $\mathbf{x} = \{x_i\}$ are two signals in $\mathbb{R}^N$ with zero mean. The normalized correlation between $\mathbf{x}$ and $\mathbf{y}$ is

$$\rho(\mathbf{x}, \mathbf{y}) = \frac{\mathbf{xy}}{\|\mathbf{x}\|\|\mathbf{y}\|}.$$

The cross-correlation over circular cross-correlation norm (CCN) between $\mathbf{x}$ and $\mathbf{y}$ is

$$c(\mathbf{x}, \mathbf{y}) = \frac{\mathbf{xy}/N}{\sqrt{\frac{1}{N-|\mathbf{A}|}\sum_{m \notin \mathbf{A}} r_{\mathbf{xy}}^2(m)}} = \frac{r_{\mathbf{xy}}(0)}{\sqrt{\frac{1}{N-|\mathbf{A}|}\sum_{m \notin \mathbf{A}} r_{\mathbf{xy}}^2(m)}}$$

where A is a small neighbor area around zero where $r_{\mathbf{xy}}(0) = (1)/(N)\mathbf{xy} = (1)/(N)\sum_{i=0}^{N-1} x_i y_i$, $|\mathrm{A}|$ is the size of A.

TABLE III
TPR OF THE DIFFERENT CI METHODS AT ZERO EXPERIMENTAL FPR WITH DIFFERENT JPEG QF

JPEG QF	Phase SPN	MLE SPN [16]	Basic SPN[3]	Model 3[9]	Model 5[9]
90	0.992	0.977	0.987	0.983	0.947
75	0.944	0.913	0.880	0.875	0.743
50	0.917	0.884	0.771	0.728	0.495

1) If $\mathbf{x}$ is independent with $\mathbf{y}$, $E(c(\mathbf{x},\mathbf{y}))=0, D(c(\mathbf{x},\mathbf{y}))=1$, where E () is the expectation operation and D () is the variance operation.
2) Let either $\mathbf{x}$ or $\mathbf{y}$ be a white noise signal (or i.i.d. vector), $(1)/(N-|\mathbf{A}|)\sum_{m\notin\mathbf{A}} r^2_{\mathbf{xy}}(m) \approx (1)/(N^3)\|\mathbf{x}\|^2\|\mathbf{y}\|^2, c(\mathbf{x},\mathbf{y}) \approx \sqrt{N}\rho(\mathbf{x},\mathbf{y}), \mathrm{PCE} = (c(\mathbf{x},\mathbf{y}))^2 \approx N\rho^2(\mathbf{x},\mathbf{y})$.

Proof: $E(x_i)=E(y_i)=0$, where E () is the expectation operation

$$\begin{aligned}
&\frac{1}{N-|\mathbf{A}|}\sum_{m\notin\mathbf{A}} r^2_{\mathbf{xy}}(m)\\
&=\frac{1}{N-\|\mathbf{A}\|}\sum_{m\notin\mathbf{A}}\left(\frac{1}{N}\sum_{i=0}^{N-1}x_i y_{i\oplus m}\right)^2\\
&=\frac{1}{N^2}\frac{1}{N-|\mathbf{A}|}\sum_{m\notin\mathbf{A}}\left(\sum_{i=0}^{N-1}x_i y_{i\oplus m}\right)^2\\
&=\frac{1}{N^2}\frac{1}{N-|\mathbf{A}|}\sum_{m\notin\mathbf{A}}\left[\sum_{i=0}^{N-1}\sum_{j=0}^{N-1}(x_i y_{i\oplus m}x_j y_{j\oplus m})\right]\\
&=\frac{1}{N^2}\sum_{i=0}^{N-1}\sum_{j=0}^{N-1}\left[(x_i x_j)\frac{1}{N-|\mathbf{A}|}\sum_{m\notin\mathbf{A}}(y_{i\oplus m}y_{j\oplus m})\right]\\
&\approx\frac{1}{N^2}\sum_{i=0}^{N-1}\sum_{j=0}^{N-1}x_i x_j E(y_{i\oplus m}y_{j\oplus m})\\
&=\frac{1}{N^2}\sum_{i=0}^{N-1}x_i^2 E\left(y^2_{i\oplus m}\right)\\
&\quad+\frac{1}{N^2}\sum_{i=0}^{N-1}\sum_{j\neq i}x_i x_j E(y_{i\oplus m}y_{j\oplus m})\\
&=\frac{1}{N^3}\sum_i x_i^2\sum_i y_i^2+\frac{1}{N^2}\times N\\
&\quad\times\sum_{m\neq 0,m=-i+1}^{N-i}r_x(m)r_y(m)\\
&=\frac{1}{N^3}\|\mathbf{x}\|^2\|\mathbf{y}\|^2+\frac{1}{N}\sum_{m=1}^{N-1}r_x(m)r_y(m).
\end{aligned}$$

1) If $\mathbf{x}$ is independent with $\mathbf{y}$

$$\begin{aligned}
E\left(r^2_{\mathbf{xy}}(0)\right)&=E\left(\left(\frac{1}{N}\sum_{i=0}^{N-1}x_i y_i\right)\left(\frac{1}{N}\sum_{j=0}^{N-1}x_j y_j\right)\right)\\
&=E\left(\frac{1}{N^2}\sum_{i=0}^{N-1}\sum_{j=0}^{N-1}(x_i y_i x_j y_j)\right)\\
&=E\left(\frac{1}{N^2}\sum_{i=0}^{N-1}x_i^2 y_i^2+\frac{1}{N^2}\sum_{i=0}^{N-1}\sum_{j\neq i}(x_i x_j y_i y_j)\right)\\
&=\frac{1}{N^2}\times N\times E\left(x_i^2\right)E\left(y_i^2\right)\\
&\quad+\frac{1}{N^2}\sum_{i=0}^{N-1}\sum_{j\neq i}E(x_i x_j)E(y_i y_j)\\
&=\frac{1}{N}E\left(x_i^2\right)E\left(y_i^2\right)+\frac{1}{N}\sum_{m=1}^{N-1}r_x(m)r_y(m)\\
&=\frac{1}{N^3}\|\mathbf{x}\|^2\|\mathbf{y}\|^2+\frac{1}{N}\sum_{m=1}^{N-1}r_x(m)r_y(m)
\end{aligned}$$

$$\begin{aligned}
E(c(\mathbf{x},\mathbf{y}))&=E\left(\frac{\mathbf{xy}/N}{\sqrt{\frac{1}{N-|\mathbf{A}|}\sum_{m\notin\mathbf{A}}r^2_{\mathbf{xy}}(m)}}\right)\\
&=\frac{E(x_i)E(y_i)}{E\left(\sqrt{\frac{1}{N-|\mathbf{A}|}\sum_{m\notin\mathbf{A}}r^2_{\mathbf{xy}}(m)}\right)}\\
&=0\\
D(c(\mathbf{x},\mathbf{y}))&=D\left(\frac{r_{\mathbf{xy}}(0)}{\sqrt{\frac{1}{N-|\mathbf{A}|}\sum_{m\notin\mathbf{A}}r^2_{\mathbf{xy}}(m)}}\right)\\
&=E\left(\frac{r^2_{\mathbf{xy}}(0)}{\frac{1}{N-|\mathbf{A}|}\sum_{m\notin\mathbf{A}}r^2_{\mathbf{xy}}(m)}\right)\\
&=1.
\end{aligned}$$

2) Let $\mathbf{y}$ be a white noise signal vector, then $r_y(m)=0, m\neq 0$

$$\begin{aligned}
&\frac{1}{N-|\mathbf{A}|}\sum_{m\notin\mathbf{A}}r^2_{\mathbf{xy}}(m)\\
&\approx\frac{1}{N^3}\|\mathbf{x}\|^2\|\mathbf{y}\|^2+\frac{1}{N}\sum_{m=1}^{N-1}r_x(m)r_y(m)\\
&=\frac{1}{N^3}\|\mathbf{x}\|^2\|\mathbf{y}\|^2.
\end{aligned}$$

Let $\mathbf{y}$ be an i.i.d. vector, $E(y_i)=0$.

$$\begin{aligned}
&\frac{1}{N-|\mathbf{A}|}\sum_{m\notin\mathbf{A}}r^2_{\mathbf{xy}}(m)\\
&\approx\frac{1}{N^3}\|\mathbf{x}\|^2\|\mathbf{y}\|^2+\frac{1}{N^2}\sum_{i=0}^{N-1}\sum_{j\neq i}x_i x_j E(y_{i\oplus m}y_{j\oplus m})\\
&=\frac{1}{N^3}\|\mathbf{x}\|^2\|\mathbf{y}\|^2+\frac{1}{N^2}\sum_{i=0}^{N-1}\sum_{j\neq i}x_i x_j E(y_i)E(y_j)\\
&=\frac{1}{N^3}\|\mathbf{x}\|^2\|\mathbf{y}\|^2.
\end{aligned}$$

Thus,

$$c(\mathbf{x},\mathbf{y}) \approx \frac{\mathbf{xy}}{\sqrt{\frac{1}{N}\|\mathbf{x}\|^2\|\mathbf{y}\|^2}} = \rho(\mathbf{x},\mathbf{y})\sqrt{N}$$
$$\mathrm{PCE} = (c(\mathbf{x},\mathbf{y}))^2 \approx N\rho^2(\mathbf{x},\mathbf{y}).$$

The proof is similar to the case of that $\mathbf{x}$ is a white noise signal (or i.i.d. vector). So let either $\mathbf{x}$ or $\mathbf{y}$ be white noise signal (or i.i.d vector), $(1)/(N-|\mathbf{A}|)\sum_{m\notin\mathbf{A}} r^2_{\mathbf{xy}}(m) \approx (1)/(N^3)\|\mathbf{x}\|^2\|\mathbf{y}\|^2, c(\mathbf{x},\mathbf{y}) \approx \sqrt{N}\rho(\mathbf{x},\mathbf{y}), \mathrm{PCE} = (c(\mathbf{x},\mathbf{y}))^2 \approx N\rho^2(\mathbf{x},\mathbf{y})$.

REFERENCES

[1] Z. Geradts, J. Bijhold, M. Kieft, K. Kurosawa, K. Kuroki, and N. Saitoh, "Methods for identification of images acquired with digital cameras," in *Proc. SPIE, Enabling Technologies Law Enforcement Security*, Feb. 2001, vol. 4232, pp. 505–512.

[2] G. C. Holst, *CCD Arrays, Cameras, and Displays*, 2nd ed. Philadelphia, PA: JCD and SPIE Press, 1998.

[3] J. Lukáš, J. Fridrich, and M. Goljan, "Digital camera identification from sensor pattern noise," *IEEE Trans. Inform. Forensics Security*, vol. 1, no. 2, pp. 205–214, Jun. 2006.

[4] Dark frame subtraction Qimage help, available [Online]. Available: http://www.ddisoftware.com/qimage/qimagehlp/dark.htm

[5] J. Lukâš, J. Fridrich, and M. Goljan, "Digital 'bullet scratches' for images," in *Proc. IEEE Int. Conf. Image Processing*, Genova, Italy, Sept. 2005.

[6] M. Goljan, M. Chen, and J. Fridrich, "Identifying common source digital camera from image pairs," in *Proc. IEEE Int. Conf. Image Processing*, San Antonio, TX, Sep. 2007, pp. 14–19.

[7] Y. Sutcu, S. Batram, H. T. Sencar, and N. Memon, "Improvements on sensor noise based source camera identification," in *Proc. IEEE Int. Conf. Multimedia Expo*, Beijing, China, Jul. 2007, pp. 24–27.

[8] M. Chen, J. Fridrich, M. Goljan, and J. Lukáš, "Determining image origin and integrity using sensor noise," *IEEE Trans. Inform. Forensics Security*, vol. 3, no. 1, pp. 74–90, Mar. 2008.

[9] C.-T. Li, "Source camera identification using enhanced sensor pattern noise," *IEEE Trans. Inform. Forensics Security*, vol. 5, no. 2, pp. 280–287, Jun. 2010.

[10] J. Fridrich, M. Chen, and M. Goljan, "Imaging sensor noise as digital x-ray for revealing forgeries," in *Proc. 9th Int. Workshop Information Hiding*, Saint Malo, France, 2007, pp. 342–358.

[11] M. Goljan and J. Fridrich, "Camera identification from cropped and scaled images," in *Proc. SPIE*, 2008, vol. 6819, pp. 681900–68190E, Electronic Imaging, Security, Steganography, and Watermarking of Multimedia Contents X.

[12] X. Kang, Y. Li, Z. Qu, and J. Huang, "Enhancing ROC performance of trustworthy camera source identification," in *Proc. SPIE*, San Francisco, CA, 2011, vol. 7880, Electronic Imaging—Media Watermarking, Security, Forensics XIII.

[13] Y. Hu, B. Yu, and C. Jian, "Source camera identification using large components of sensor pattern noise," in *Proc. 2nd Int. Conf. Computer Science Applic. (CSA'09)*, Jeju, South Korea, Dec. 2009, pp. 1–5.

[14] Y. Hu, C. Jian, and C.-T. Li, "Using improved imaging sensor pattern noise for source camera identification," in *Proc. IEEE Int. Conf. Multimedia Expo (ICME)*, 2010, pp. 1481–1486.

[15] A. Swaminathan, M. Wu, and K. J. R. Liu, "Nonintrusive component forensics of visual sensors using output images," *IEEE Trans. Inform. Forensics Security*, vol. 2, no. 1, pp. 91–106, Mar. 2007.

[16] M. Goljan, J. Fridrich, and T. Filler, "Large scale test of sensor fingerprint camera identification," in *Proc. SPIE*, San Jose, CA, Jan. 18–22, 2009, vol. 7254, pp. 0I 1–0I 12, Electronic Imaging, Media Forensics and Security XI.

[17] M. Goljan, J. Fridrich, and T. Filler, "Managing a large database of camera fingerprints," in *Proc. SPIE*, San Jose, CA, Jan. 17, 2010, vol. 7541, pp. 08-01–08-12, Electronic Imaging, Media Forensics and Security XII.

[18] M. Goljan and J. Fridrich, "Digital camera identification from images—Estimating false acceptance probability," in *Proc. 8th Int. Workshop Digital Watermarking*, Busan, Korea, Nov. 10–12, 2008.

[19] H. Cao and A. C. Kot, "Mobile camera identification using demosaicing features," in *Proc. ISCAS*, 2010, pp. 1683–1686.

[20] M. K. Mihcak, I. Kozintsev, and K. Ramchandran, "Spatially adaptive statistical modeling of wavelet image coefficients and its application to denoising," in *Proc. IEEE Int. Conf. Acoustics, Speech, Signal Processing*, Phoenix, AZ, Mar. 1999, vol. 6, pp. 3253–3256.

Xiangui Kang (M'00) received the B.S. degree from Peking University, in 1990, the M.S. degree from Nanjing University, in 1993, and the Ph.D. degree from Sun Yat-Sen University, Guangzhou, China, in 2004.

He is currently a Professor with the School of Information Science and Technology, Sun Yat-Sen University, Guangzhou, China. His research interests include information forensics, watermarking, multimedia communications and security.

Dr. Kang is a member of the IEEE ComSoc's Multimedia Communications Technical Committee.

Yinxiang Li received the B.S. and M.S. degrees in software engineering from Sun Yat-Sen University, Guangzhou, China, in 2009 and 2011, respectively.

His research interests include image forensics and information security.

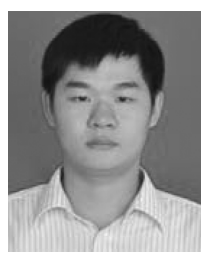

Zhenhua Qu received the B.S. degree from Tsinghua University, P. R. China, in computer science and technology, and the Ph.D. degree from Sun Yat-Sen University, P. R. China, in communication and information systems.

He joined Guangzhou Research Institution of China Telecom in 2011 and is still with Sun Yat-Sen University. His research interests include image processing, multimedia security, pattern recognition, and in particular digital image forensics.

Jiwu Huang (SM'00) received the B.S. degree from Xidian University, China, in 1982, the M.S. degree from Tsinghua University, China, in 1987, and Ph.D. degree from Institute of Automation, Chinese Academy of Science, in 1998.

He is currently a Professor with the School of Information Science and Technology, Sun Yat-Sen University, Guangzhou, China. His current research interests include multimedia security and data hiding.

Dr. Huang serves as a member of IEEE CAS Society Technical Committee of Multimedia Systems and Applications and the chair of IEEE CAS Society Guangzhou chapter.